Journal of Photochemistry and Photobiology A: Chemistry 133 (2000) 83–88

Journal of Photochemistry and Photobiology A:Chemistry

www.elsevier.nl/locate/jphotochem

ESR spin-trapping detection of radical intermediates in the TiO_2-assisted photo-oxidation of sulforhodamine B under visible irradiation

Guangming Liu [a], Jincai Zhao [a,*], Hisao Hidaka [b]

[a] The Laboratory of Photochemistry, Center for Molecular Science, Institute of Chemistry, The Chinese Academy of Sciences, Beijing 100080, China
[b] Frontier Research Center for the Earth Environment Protection, Meisei University, 2-1-1 Hodokubo, Hino, Tokyo 191, Japan

Received 1 September 1999; received in revised form 24 January 2000; accepted 25 January 2000

Abstract

The ESR spin-trapping technique using 5,5-dimethyl-1-pyrroline-*N*-oxide (DMPO) and *N*-*t*-butyl-α-phenyl-nitrone (PBN) as spin-trap reagents has been applied to detect free radical intermediates generated during the in situ visible irradiation of aqueous sulforhodamine B (SRB)–TiO_2 air-saturated dispersion. Hydroxyl radical ($^{\bullet}OH$), hydroperoxyl radical ($HO_2^{\bullet}$) and hydrated electrons (e_{aq}^{-}) were detected in the TiO_2-assisted photo-oxidation of SRB under visible irradiation. The mechanism for the generation of active oxygen radicals and the role of these photogenerated active oxygen radicals in the photo-oxidation process are discussed. It is suggested that the oxygen molecules rather than these active oxygen radicals are the main oxidizing agent and play an important role in the visible photo-oxidation of SRB mediated by TiO_2 particles. © 2000 Elsevier Science S.A. All rights reserved.

Keywords: ESR spin-trapping; TiO_2; Visible light; Photo-oxidation; DMPO; PBN

---

1. Introduction

Photocatalytic reactions with semiconductor particles have been paid much interest because of their possible applications to solar storage and treatment of wastewater [1–4]. In order to investigate the mechanism of photocatalytic reactions, it is important to monitor intermediate radicals. ESR spectroscopy offers an ideal method for the study of this type of interfacial photoreaction. A spin-trapping technique has been used to observe directly active radical intermediates and provides essential information for understanding the reaction mechanisms. For example, Noda and coworkers [5,6] detected active oxygen radicals in the UV light photoexcited TiO_2 aqueous dispersions, in aqueous H_2O_2 solutions, and in non-aqueous solvents by ESR spin-trapping techniques. Nosaka et al. [7] observed methyl radicals in the photo-Kolbe reaction by means of in situ measurements with flow-electron spin resonance for deuterated acetic acid and deduced two reaction paths for the methyl radical formation.

Recently, we have focused much attention on the photodegradation of dye pollutants in aqueous TiO_2 dispersions under *visible light irradiation* [8–14]. The visible irradiation mechanism may involve the following processes: the dye rather than TiO_2 particles is excited by visible light, the excited dyes inject electrons into the conduction band of TiO_2 particles to form dye cationic radicals. The conduction band electrons are scavenged by preadsorbed molecular oxygen to yield the superoxide radical anions, $O_2^{\bullet -}$, which produce $HO_2^{\bullet}$ radicals on protonation ($pK_a=4.69$) [15]. H_2O_2 can be formed by disproportionation of $HO_2^{\bullet}$ and/or reduction of superoxide [15], and can be further reduced to produce the hydroxyl radicals. However, it still remains an unsettled question as to how the radical intermediates are generated in the primary steps and how the active oxygen radicals and molecular oxygen work in the photocatalytic reaction. The application of ESR spin-trapping techniques appears to be one of the promising approaches for the detection of radicals produced and can serve as a very valuable tool in gaining a better understanding of the reaction mechanisms on semiconductor surfaces.

We report here the results involving spin-trapping of short-lived radical intermediates produced during the in situ visible irradiation of sulforhodamine B (SRB)–TiO_2 dispersions with two spin traps: 5,5-dimethyl-1-pyrroline-*N*-oxide (DMPO) and *N*-*t*-butyl-α-phenyl-nitrone (PBN). The exper-

---

[*] Corresponding author. Present address: Institute of Photographic Chemistry, The Chinese Academy of Sciences, Beijing 100101, China.
Fax: +86-10-6487-9375.
E-mail address: jczhao@ipc.ac.cn (J. Zhao)

PII: S1010-6030(00)00227-6

imental results demonstrate the production of intermediates of hydroxyl ($^{\bullet}OH$), hydroperoxyl ($^{\bullet}OOH$) radicals and hydrated electrons (e^{-}_{aq}) in the photoprocess. The role of active oxygen radicals and oxygen molecules in the process are also discussed.

2. Experimental section

2.1. Materials

TiO_2 (P25, ca. 80% anatase, 20% rutile; BET area, ca. $50\,m^2\,g^{-1}$) was kindly supplied by Degussa. The spin traps DMPO and PBN were purchased from Sigma. The dye SRB was laser grade and other chemicals were all of analytical reagent grade quality and used without further purification. Deionized and doubly distilled water was used throughout this study. The pH of the solution was not adjusted and kept its original value (pH 4.0).

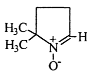

DMPO

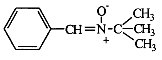

PBN

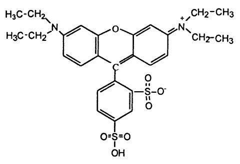

Sulforhodamine B

3. Procedures and analyses

3.1. UV–Vis spectra

A 500 W halogen lamp (Institute of Electric Light Source, Beijing) was used as the light source and positioned inside a cylindrical Pyrex vessel surrounded by a circulating water jacket (Pyrex) to cool the lamp. A cutoff filter was also placed outside the Pyrex jacket to completely remove radiation below 410 nm and to ensure irradiation of the dispersion only by visible light wavelengths. SRB aqueous solution (usually 50 ml) with or without a known amount of TiO_2 powder was put in a Pyrex cell. Prior to irradiation, the suspensions were stirred in the dark for ca. 30 min to ensure establishment of an adsorption–desorption equilibrium of dye on the TiO_2 surface. After illumination for appropriate periods, the TiO_2 powder was separated off by centrifuging and filtration (Millipore filter: pore size 0.22 μm). UV–Vis spectra of the degraded solution were recorded by a Lambda Bio 20 spectrophotometer (Perkin–Elmer).

3.2. ESR measurements

Electron paramagnetic resonance (ESR) signals of paramagnetic species spin-trapped with DMPO and PBN were recorded at ambient temperature (298 K) with a Brucker ESP 300E spectrometer; the irradiation source (λ=532 nm) was a Quanta-Ray Nd:YAG pulsed (10 pulses per second) laser system. The settings for the ESR spectrometer were center field=3486.70 G; sweep width=100.0 G; microwave frequency=9.82 GHz; modulation frequency=100 kHz and power=5.05 mW. To minimize measurement errors, the same quartz capillary tube was used throughout for ESR measurements. The ESR spectrometer was coupled to a computer for data acquisition and instrument control. The control experiments established that no light-induced radicals were obtained in the absence of the dye. Magnetic parameters of the radicals detected were obtained from direct measurements of magnetic field and microwave frequency.

4. Results and discussion

4.1. DMPO spin-trapping

The dye SRB can be strongly adsorbed on the TiO_2 surface, which is reflected by a ca. 30.1% decrease in absorbance of UV–Vis spectrum in inset a of Fig. 6 (spectrum 2). Fig. 1 shows that addition of DMPO (2.5×10^{-2} M) to O_2-saturated aqueous solutions of SRB (2×10^{-4} M) in the presence of TiO_2 ($2\,g\,l^{-1}$), followed by in situ light irradiation of the visible laser at λ=532 nm, gave rise to a sequence of ESR spectra. It is obvious that the spectra of Fig. 1 are composed of the signals due to two kinds of spin adducts. The first of those can be easily identified as the characteristic DMPO–$^{\bullet}OH$ adduct with a peak intensity of 1:2:2:1 (indicated by asterisks). The second species is characterized by having an odd number of peaks (i.e. it is symmetrical around the central signal), showing that the unpaired electron must be interacting with either a single nitrogen or a single nitrogen and even number of hydrogen atoms. The most likely candidate for this species is the reduced forms of the spin trap (DMPO–$^{\bullet}H$).

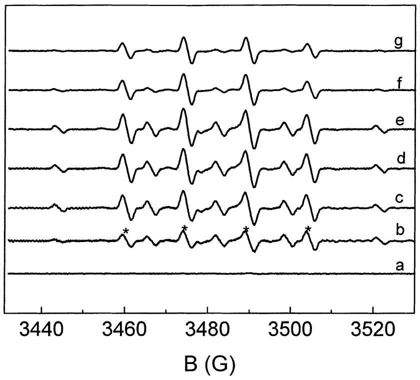

Fig. 1. DMPO spin-trapping ESR spectra of SRB–TiO_2 dispersions under laser irradiation at λ=532 nm. Spectra a–e denote the irradiation times 0, 1, 2, 3, 4 min, respectively, and f and g show the decay of spectrum e in the dark for 1 and 3 min, respectively (asterisks denote the position of hyperfine peaks of DMPO–$^{\bullet}OH$ adduct).

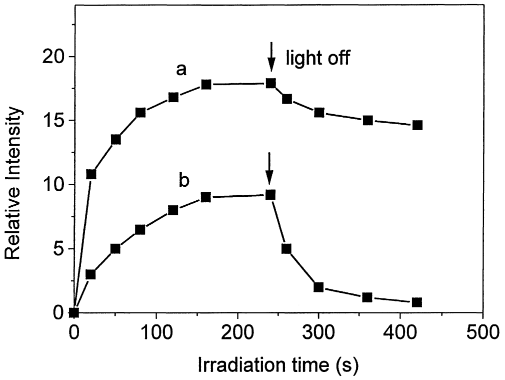

Fig. 2. Kinetics of the build up and decay of DMPO–$^{\bullet}$OH (curve a) and DMPO–$^{\bullet}$H adducts (curve b).

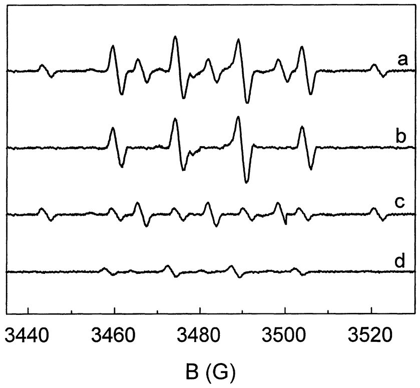

Fig. 3. (a) ESR spectrum obtained after irradiation of an O_2-saturated SRB–TiO_2 dispersion for 4 min under the same conditions as in Fig. 1; (b) spectrum after decay of spectrum a for 2 min in the dark; (c) spectrum obtained by spectrum a minus spectrum b; (d) spectrum obtained in the absence of TiO_2.

The DMPO–$^{\bullet}$OH adduct decayed much slowly after turning off the irradiation light and could be still detected for several hours in the dark. On the other hand, the DMPO–$^{\bullet}$H adduct decayed rapidly and it has been proven to be relatively unstable [16] when the visible light irradiation is interrupted, as shown in Figs. 1 and 2. The time dependence of the radical concentrations was traced in order to investigate the reaction behaviors of the spin adducts. For efficiently trapping the radicals produced, sufficient DMPO (2.5×10^{-2} M) was added to minimize competing reactions of radicals with the dye SRB (2×10^{-4} M). Fig. 2 shows the build up of DMPO–$^{\bullet}$H and DMPO–$^{\bullet}$OH to the steady state when the light is turned on and its subsequent decay when the light is turned off for an SRB–TiO_2 dispersion containing DMPO under irradiation by laser light of 532 nm. The intensities increased with the irradiation time and achieved the steady state at 160 s of irradiation, indicating an equilibrium between the production of radicals' adducts and the extinction of radicals' adducts. The signal intensities leveled off when the irradiation was stopped. The decay of signals for DMPO–$^{\bullet}$H and DMPO–$^{\bullet}$OH follows apparent second-order kinetics, with the ratio of rate constants ($k_{\text{DMPO–}^{\bullet}\text{H}}/k_{\text{DMPO–}^{\bullet}\text{OH}} = 60$), indicating that termination is through a radical–radical reaction and the decay of DMPO–$^{\bullet}$H is faster than that of DMPO–$^{\bullet}$OH.

The intensity of signals of hydroxyl radicals observed in the absence of TiO_2 (spectrum d of Fig. 3) was negligible compared to that in the presence of TiO_2 (spectrum a of Fig. 3), indicating the important role of TiO_2 in the formation of hydroxyl radical and the hydroxyl radicals observed in Fig. 1 in the presence of TiO_2 mainly arising from the photocatalytic process and not from the photoionization of the dye (as noted below). Fig. 3c depicts the ESR spectrum for only the DMPO–$^{\bullet}$H adduct obtained by subtracting the spectrum at 2 min after turning off the light (Fig. 3b) from the spectrum of 4 min irradiation (Fig. 3a). The DMPO–$^{\bullet}$H shows the nine peaks with an intensity ratio of 1:1:2:1:2:1:2:1:1, whose splitting pattern is well reproduced by HFSC values of a_N=16.6 G and a_H^{β}=22.6 G. Magnetic parameters determined for DMPO–$^{\bullet}$H are in good agreement with those reported previously [17–19].

DMPO is an excellent scavenger not only for the hydroxyl radical ($k(^{\bullet}\text{OH}+\text{DMPO})=4.3\times10^{9}\ \text{M}^{-1}\,\text{s}^{-1}$) [20] but also for hydrated electrons ($k(e_{aq}^{-}+\text{DMPO})=1.5\times10^{10}\ \text{M}^{-1}\,\text{s}^{-1}$) and hydrogen atoms [21]. Hence, the DMPO–$^{\bullet}$H adduct may arise from the trapping of a hydrogen atom or by the reaction of the hydrated electron with the spin trap followed by

$$\text{DMPO} + {}^{\bullet}\text{H} \rightarrow \text{DMPO–}{}^{\bullet}\text{H} \tag{1}$$

$$\text{DMPO} + e_{aq}^{-} + \text{H}^{+} \rightarrow \text{DMPO–}{}^{\bullet}\text{H} \tag{2}$$

protonation. We used N_2O to distinguish between these two mechanisms because it is known to effectively react with e_{aq}^{-} ($k(e_{aq}^{-}+\text{N}_2\text{O})=8.7\times10^{9}\ \text{M}^{-1}\,\text{s}^{-1}$) but not with $^{\bullet}$H at neutral pHs [22] as in Eq. (3):

$$e_{aq}^{-} + \text{N}_2\text{O} + \text{H}^{+} \rightarrow \text{N}_2 + {}^{\bullet}\text{OH} \tag{3}$$

The concentration of N_2O is 2.2×10^{-2} M in a saturated solution at 298 K. The results clearly show that N_2O saturation significantly decreased the ESR signals of DMPO–$^{\bullet}$H (spectrum b in Fig. 4), which indicates that radical formation occurs mainly via reaction (2) but not via reaction (1). The ESR signals of the hydrated electrons were relatively decreased in the absence of TiO_2 particles as compared to that observed in the presence of TiO_2 (spectrum d in Fig. 3). Therefore, it is concluded that the hydrated electrons may come from the conduction band electrons injected by the excited dye and from the direct photoionization of the dye SRB. The hydrated electron that resulted from the visible-laser induced photoionization of dyes is also reported in the case of Acid Orange 7 [23]. We also found that the N_2-saturation of the solution depressed the ESR signal for the adduct of the hydroxyl radical with DMPO (spectrum d in Fig. 4). This fact indicates that the hydroxyl radical is derived from molecular O_2. On the other hand, a small amount of DMPO–$^{\bullet}$OH

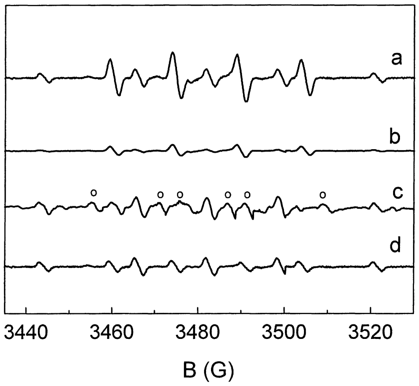

Fig. 4. (a) ESR spectrum obtained after irradiation of an O_2-saturated SRB–TiO_2 dispersion for 4 min under the same conditions as in Fig. 1; (b) spectrum obtained by irradiation of an N_2O saturated SRB–TiO_2 dispersion for 4 min under the otherwise identical conditions; (c) in the presence of ethanol (0.2 M); (d) spectrum obtained by irradiation of an N_2-saturated SRB–TiO_2 dispersion.

adducts in the N_2O-saturated solution is due to the hydroxyl radical formed via the reaction in Eq. (3), as depicted in Fig. 4 (spectrum b).

The signal intensity of hydroxyl radicals in the visible irradiated dye–TiO_2 dispersion was insensitive to superoxide dismutase (SOD) (30 $\mu g\, ml^{-1}$) which catalytically converts the superoxide radical anion to H_2O_2 and O_2, ruling out the possibility of $^{\bullet}OH$ radical signals resulting from decomposition of a DMPO–superoxide adduct. The radical was quenched by addition of hydroxyl radical scavengers such as ethanol (0.2 M) (spectrum c in Fig. 4) (open circles denote signals of DMPO–$^{\bullet}CH(CH_3)OH$ adduct [5]), suggesting the direct addition of hydroxyl radical to DMPO. In order to examine whether hydroxyl radical generation takes place via reduction of H_2O_2 produced in the system, ESR experiments were performed in the presence of catalase enzyme, which catalytically converts the H_2O_2 to H_2O and O_2. The signals of DMPO–$^{\bullet}OH$ adduct disappeared after addition of catalase (400 μl, 2 $mg\, ml^{-1}$) into the system, and on the contrary, it increased after addition of external H_2O_2, which suggests that the $^{\bullet}OH$ radical originates from the reduction of H_2O_2 formed in the photo-oxidation process (Eq. (8)). Both the conduction band electrons (injected by the excited dye) and the hydrated electrons can be effectively scavenged by oxygen ($k(e_{aq}^{-}+O_2)=1.9\times10^{10}\ M^{-1}\, s^{-1}$) [22] and further reduced or disproportionated to H_2O_2 via Eqs. (4)–(7). Finally, the hydroxyl radicals may be produced from H_2O_2 as given in Eq. (8). As superoxide and H_2O_2 can be reduced by both hydrated electrons (e_{aq}^{-}) and conduction band electrons (e_{cv}^{-}), we use e (the total electrons, including e_{aq}^{-} and e_{cv}^{-}) in Eq. (7) and (8):

$$O_2 + e_{aq}^{-}(\text{or } e_{cv}^{-}) \rightarrow O_2^{\bullet -} \tag{4}$$

$$H^{+} + O_2^{\bullet -} \leftrightarrow HO_2^{\bullet} \quad pK_a = 4.69 \quad [15] \tag{5}$$

$$HO_2^{\bullet} + HO_2^{\bullet} \rightarrow O_2 + H_2O_2$$
$$K = 8.6\times10^{5}\ M^{-1}\, s^{-1} \quad [15] \tag{6}$$

$$O_2^{\bullet -} + e + 2H^{+} \rightarrow H_2O_2 \tag{7}$$

$$H_2O_2 + e \rightarrow {}^{\bullet}OH + OH^{-} \tag{8}$$

Although superoxide should be formed as a result of the scavenging of the electron by O_2, we were unable to detect directly the spin-adduct of this radical with DMPO under the present conditions because the facile disproportionation reaction of superoxide in water [15] precludes any slow reactions between $O_2^{\bullet -}$ or $HO_2^{\bullet}$ and DMPO (k=10 and $6.6\times10^{3}\ M^{-1}\, s^{-1}$, respectively) [24].

4.2. *Spin trapping by PBN*

A comparison of the data that were obtained from experiments using two or more spin-trap reagents is profitable for assigning the produced intermediates. Fig. 5 shows the ESR spectra of the visible light irradiated SRB–TiO_2–PBN aqueous and methanol dispersions at room temperature. The intensity of the spin adduct of PBN was stronger than those of the DMPO spin adducts. The PBN is more sensitive than DMPO in trapping the active oxygen radicals. The signal in spectrum a can be assigned to PBN spin adducts of the hydroxyl radicals with HFSC values of a_N=15.10 G and a_H^{β}=2.75 G. These HFSC values correspond well to previously reported values for the spin adducts [25–27]. The signal of PBN–$^{\bullet}H$ adducts (a triplet of triplets, a_N=14.98 G and a_H^{β}=7.50 G [28]) was not observed in the system, probably due to the lower ability of PBN in trapping hydrated electrons compared to that of DMPO. In order to confirm the hydroxyl radical production in the system, methanol (1%) was added to the aqueous SRB–TiO_2–PBN dispersion instead of EtOH that was used in the DMPO system (as noted above) because both MeOH and EtOH can be used as hydroxyl radical scavengers, which were added to the disper-

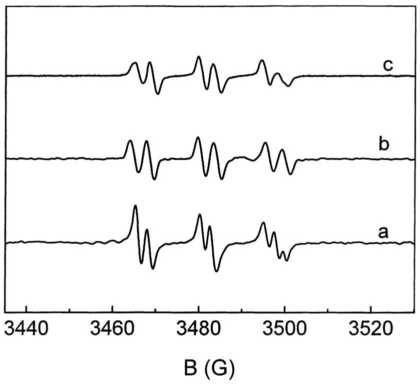

Fig. 5. ESR spectra of the PBN spin adducts obtained by visible photoexcitation of SRB–TiO_2 dispersions in different solvents. (a) H_2O; (b) H_2O+CH_3OH (1%); (c) CH_3OH.

sion to confirm the hydroxyl radical production [13], and moreover, we carried out subsequent ESR experiments in which the ratio of CH_3OH to H_2O in the mixed solvent system was varied to ascertain the generation of the superoxide radical. If the hydroxyl radical is produced, we would expect $^{\bullet}CH_2OH$ radical formation [29]. As depicted in Fig. 5b, the PBN–$^{\bullet}CH_2OH$ adduct was indeed observed with a_N=15.50 G and a_H^{β}=3.70 G [29]. As in the case of aqueous SRB–TiO_2 with DMPO spin trap, neither $O_2^{\bullet -}$ nor $HO_2^{\bullet}$ were observed in the case of PBN in water. This is because the concentrations of $O_2^{\bullet -}$ and $HO_2^{\bullet}$ are not high enough to be detected by ESR owing to rapid dismutation reaction in water [30]. However, superoxide is relative stable in non-aqueous solvents because the disproportionation to give the peroxide diaion O_2^{2-} is highly unfavorable in such solvents [15]. Therefore, we carried out subsequent ESR experiments in which CH_3OH was used as the solvent and PBN was employed as a spin trap to observe the generation of the superoxide radical. As illustrated in Fig. 5c, only small signals of PBN–$^{\bullet}OOH$ adducts (a triplet of doublets with HFSC values of a_N=14.80 G and a_H^{β}=2.75 G) [6,31] were obtained on irradiating a metholic SRB–TiO_2 dispersion under the identical conditions as above. When a small amount of water was injected into the dispersion, the magnitude of the ESR signals increased immediately. As more water was added, the signal first increased gradually and then slowly decreased. Since PBN can trap $HO_2^{\bullet}$ but not trap $O_2^{\bullet -}$ [32], the small signal observed initially was probably due to the presence of a small amount of residual water and protonation of $O_2^{\bullet -}$ to produce trappable $HO_2^{\bullet}$, while the signal intensity decreased after reaching the maximum value owing to the disproportionation of $HO_2^{\bullet}$ as more water was added. Thus, the results observed from experiments using PBN nicely support those obtained from experiments using DMPO.

ESR results of spin adducts of $^{\bullet}OH$ and $HOO^{\bullet}$ indicate the existence of radical intermediates during the photo-oxidation of the dye under visible irradiation. The presence of the $HOO^{\bullet}$ spin adduct leads to speculation that molecular O_2 adsorbed on TiO_2 semiconductor powders may be preferentially reduced when the dye SRB is excited by visible light and injects an electron into the conduction band of TiO_2. The superoxide radical continues to be reduced by conduction band electrons or is disproportionated to form H_2O_2. The H_2O_2 produced could provide a possible source of $^{\bullet}OH$ via a reduction reaction. In order to clarify the role of these active oxygen radicals in the process, sufficient DMPO was added into the dispersion to observe the influence on the photo-oxidation of SRB in the following experiments.

UV–Vis spectral changes of SRB (2×10^{-5} M) versus irradiation time in the presence of TiO_2 (100 mg) under visible irradiation is shown in inset a of Fig. 6. Visible irradiation of the aqueous SRB–TiO_2 dispersion led to a decrease in absorption concomitantly with a shift of the band to shorter wavelengths. Similar hypsochromic shifts was reported by Watanabe et al. [33] in the Rhodamine B–CdS system causing by *N*-de-ethylation of Rhodamine B. It indicates that competitive reactions between de-ethylation and cleavage of the SRB chromophore ring structure occur, with the cleavage of chromophore structure predominating, during the photo-oxidation of SRB. Fig. 6b shows the irradiation effect on the UV–Vis spectrum of the dispersion with DMPO (1.6×10^{-3} M). In this case, the active oxygen produced is trapped by DMPO and it forms relatively stable spin adducts. The spectrum in the presence of DMPO also decreases in intensity, while no band shift was observed. Curve a in Fig. 6 shows the temporal concentration changes of SRB under the same conditions as in inset a of Fig. 6, illustrating apparent first-order kinetics with an initial rate constant $k=1.68\times10^{-2}$ min^{-1}. Curves b and c show the temporal concentration changes of SRB under identical conditions except for in the presence of DMPO (1.6×10^{-3} M) and DMPO (4.0×10^{-3} M), respectively. It indicates that the addition and the concentration changes of DMPO have little effect on the initial rate of photo-oxidation of SRB in at least the first 30 min and that the latter degradation process is hindered. This fact probably arises from the influence of spin adducts of DMPO and the intermediates produced on the adsorption of the dye SRB on the TiO_2 surface. From the above results, we can infer that *N*-de-ethylation may result from the reaction between the dye radical cation and the active oxygen radicals (hydroxyl and/or superoxide radicals) and that the destruction of the dye chromophore structure results from the reaction between the dye radical cation and oxygen molecules independent of the active oxygen radicals.

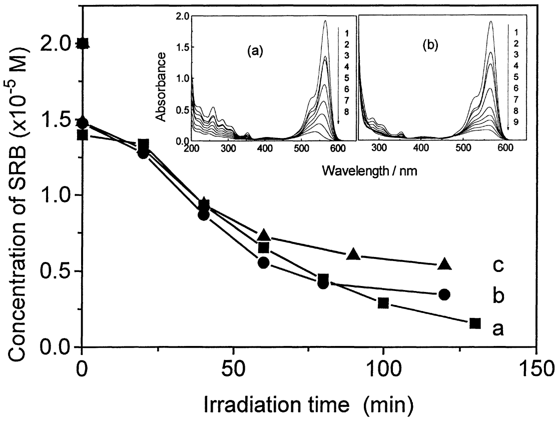

Fig. 6. The temporal changes of SRB concentrations (2×10^{-5} M, 50 ml; TiO_2: 100 mg) vs. irradiation time. Curve a: in the absence of DMPO; curve b: in the presence of DMPO (1.6×10^{-3} M); curve c: in the presence of DMPO (4.0×10^{-3} M). Inset a: UV–Vis spectra changes of SRB (2×10^{-5} M, 50 ml; TiO_2: 100 mg) as a function of irradiation time; spectra 2, 3, 4, 5, 6, 7 and 8 denote the irradiation time 0, 20, 40, 60, 80, 100 and 130 min, respectively. Spectrum 1 is the UV–Vis spectrum of SRB before the addition of TiO_2 particles to the solution. Inset b: UV–Vis spectra changes of SRB (2×10^{-5} M, 50 ml; TiO_2: 100 mg) as a function of irradiation time after addition of DMPO (1.6×10^{-3} M); spectra 2, 3, 4, 5, 6, 7, 8 and 9 denote the irradiation time 0, 20, 40, 60, 80, 120, 225 and 315 min, respectively. Spectrum 1 is the UV–Vis spectrum of SRB before the addition of TiO_2 particles to the solution.

5. Conclusions

The ESR spin-trapping techniques have been used to detect paramagnetic species and reactively short-lived radicals formed during 532 nm laser irradiation of the SRB–TiO_2 dispersions. Active oxygen radicals (hydroperoxyl and hydroxyl radicals) were detected in irradiated TiO_2–SRB dispersions with DMPO and PBN as spin traps. The hydrated electron, e^-_{aq}, was trapped by DMPO and detected as the DMPO–$^\bullet$H adduct. The generation of the active oxygen radicals is ascribed to continuous reduction of molecular oxygen by the conduction band electrons. Molecular oxygen adsorbed on the TiO_2 surface is the primary photochemical oxidizing agent, resulting in the photo-oxidation of the dye SRB by reacting with $SRB^{\bullet+}$ when the excited dye injects one electron into the conduction band of TiO_2 under visible irradiation.

Acknowledgements

The generous financial support of this work from the National Natural Science Foundation of China (No. 29725715, No. 59772033, No. 29637010), the Foundation of the Chinese Academy of Sciences and the China National Committee for Science and Technology is gratefully acknowledged. The work in Tokyo is sponsored by a Grant-in-Aid for Scientific Research from the Japanese Ministry of Education (No. 10640569; to H.H). We are also grateful to Prof. J. Chen for her assistance in measurements of the ESR spectra.

References

[1] E. Pelizzetti, M. Schiavello (Eds.), Photochemical Conversion and Storage of Solar Energy, Kluwer Academic Publishers, Dordrecht, The Netherlands, 1991.
[2] M.A. Fox, M.T. Dulay, Chem. Rev. 93 (1993) 341.
[3] D.F. Ollis, E. Pelizzetti, N. Serpone, Environ. Sci. Technol. 25 (1991) 1522.
[4] M.R. Hoffmann, S.T. Martin, W. Choi, D.W. Bahnemann, Chem. Rev. 95 (1995) 69.
[5] H. Noda, K. Oikawa, H. Kamada, Bull. Chem. Soc. Jpn. 65 (1992) 2505.
[6] H. Noda, K.H. Nishiguchi, H. Kamada, Bull. Chem. Soc. Jpn. 66 (1993) 3542.
[7] Y. Nosaka, K. Koenuma, K. Ushida, A. Kira, Langmuir 12 (1996) 736.
[8] F. Zhang, J. Zhao, L. Zang, T. Shen, H. Hidaka, E. Pelizzetti, N. Serpone, J. Mol. Catal. A: Chem. 120 (1997) 173.
[9] F. Zhang, J. Zhao, T. Shen, H. Hidaka, E. Pelizzetti, N. Serpone, Appl. Catal. B: Environ. 15 (1998) 147.
[10] J. Zhao, K. Wu, T. Wu, H. Hidaka, N. Serpone, J. Chem. Soc., Faraday Trans. 94 (1998) 673.
[11] T. Wu, G. Liu, J. Zhao, H. Hidaka, N. Serpone, J. Phys. Chem. B 102 (1998) 5845.
[12] J. Zhao, T. Wu, K. Wu, K. Oikawa, H. Hidaka, N. Serpone, Environ. Sci. Technol. 32 (1998) 2394.
[13] T. Wu, T. Lin, J. Zhao, H. Hidaka, N. Serpone, Environ. Sci. Technol. 33 (1999) 1379.
[14] G. Liu, T. Wu, J. Zhao, H. Hidaka, N. Serpone, Environ. Sci. Technol. 33 (1999) 2081.
[15] D.T. Sawyer, J.S. Valentine, Acc. Chem. Res. 14 (1981) 393.
[16] M.J. Davies, T.F. Slater, Biochem. J. 240 (1986) 789.
[17] A.S.W. Li, C.F. Chignell, J. Biochem. Biophys. Methods 22 (1991) 83.
[18] C.F. Chignell, A.G. Motten, R.H. Sik, C.E. Parker, K. Reszka, Photochem. Photobiol. 59 (1994) 5.
[19] F.P. Sargent, E.M. Gardy, Can. J. Chem. 52 (1974) 3645.
[20] P. Neta, S. Steenken, E.G. Janzen, R.V. Shetty, J. Phys. Chem. 84 (1980) 532.
[21] B. Kalyanaraman, C.C. Felix, R.C. Sealy, Photochem. Photobiol. 36 (1982) 5.
[22] M. Anbar, M. Babenek, A.B. Ross, Natl. Stand. Ref. Data Ser., Nat. Bur. Stand. 43 (1973) 23.
[23] K. Vinodgopal, P.V. Kamat, J. Photochem. Photobiol. A: Chem. 83 (1994) 141.
[24] E. Finkelstein, G.M. Rosen, E.J. Rauckman, J. Am. Chem. Soc. 102 (1980) 4993.
[25] J.R. Harbour, V. Chow, J.R. Bolton, Can. J. Chem. 52 (1974) 3549.
[26] C.D. Jaeger, A.J. Bard, J. Phys. Chem. 83 (1979) 3146.
[27] J.R. Harbour, J.R. Bolton, Biochem. Biophys. Res. Commun. 64 (1975) 803.
[28] E.G. Janzen, D.E. Nutter, E.R. Davis, B.J. Blackburn, J.L. Poyer, P.B. McCay, Can. J. Chem. 56 (1978) 2239.
[29] A.N. Saprin, L.H. Piette, Arch. Biochem. Biophys. 180 (1977) 480.
[30] J.M. Mccord, I. Fridovich, J. Biol. Chem. 244 (1969) 6049.
[31] G.R. Buettner, Free Radical Biol. Med. 3 (1987) 259.
[32] E.G. Janzen, B.J. Blackburn, J. Am. Chem. Soc. 91 (1969) 4481.
[33] T. Watanabe, T. Takizawa, K. Honda, J. Phys. Chem. 81 (1977) 1845.